Transaction B: Mechanical Engineering
Vol. 16, No. 4, pp. 291–300
© Sharif University of Technology, August 2009

SCIENTIA IRANICA

Some Experimental Studies on the Performance of a Rigid Wing Land Yacht Model in Comparison with VPP

M. Khayyat[1,*] and M. Rad[1]

Abstract. *It is important to understand the flow characteristics and performance of wings for designers who want to have an efficient thrust in a land yacht. In this paper, a comparison of aerodynamic forces obtained by testing the land yacht model in a wind tunnel and by the Velocity Prediction Program (VPP) is presented. The wind tunnel testing of a land yacht is an effective design tool, but at present it is mainly used for VPP validation, which allows for a faster and more efficient design process. The rigid wing land yacht model, which is a radio controlled model, is tested in the national open jet wind tunnel of the Malek Ashtar University of Technology in Iran. The wing data, which is obtained from the wind tunnel, is used in the VPP as input data and then the parasitic drag and aerodynamic forces that are measured in the wind tunnel are compared to those in the VPP. Comparison of the results shows a reasonably good agreement between experimental data and VPP data. So the latter can be used as an effective tool in the design of a land yacht.*

Keywords: *Land yacht; Wind tunnel; Aerodynamic; Wing.*

INTRODUCTION

In the early 1970s researchers at the Massachusetts Institute of Technology (MIT) were funded to produce a methodology that would predict the speed of a sailing yacht, given knowledge of its hull, rig and sail plan geometry [1]. Thus, the H. Irving Pratt project produced the first Velocity Prediction Program (VPP). In 1976, the Offshore Committee of the U.S. Sailing adopted this computer program as the basis of a Measurement Handicapping System (MHS) to facilitate the equitable handicapping of driver type boats. Finally, in November 1985, the International Measurement System (IMS) became the only internationally administered handicap rule [1,2]. From IMS roots, several sophisticated VPP programs have been developed and these offer not only enhanced usability but also more comprehensive force models together with the ability to accept force data from experimental results. But, all of these VPP programs are for sailing yachts and there is no accurate VPP program for rigid wing land yachts. However, a large number of designers and researchers maintain their own 'in house' performance prediction software, without much confidence [3].

Velocity Prediction Programs (VPPs) in land yachts predict the performance of a land yacht by balancing the aerodynamic forces and moments so that the vehicle is in equilibrium. The aerodynamic force and moment coefficients used by a VPP are determined in a number of ways using theoretical models, Computational Fluid Dynamics (CFD) or experimental methods. Obtaining lift and drag coefficients from a wind tunnel is complicated and expensive, but it is accurate. In this research, we have used the latter. The wing tuning, i.e. the direction of a wing, should be altered to meet oncoming wind at appropriate angles to push a land yacht towards a destination with the best efficiency. Normally, this tuning is performed by land yacht drivers, but designers should also make the wings produce a good performance at the design stage. In order to design an efficient wing system, the designer is forced to have information about the essential characteristics of a wing system. This paper presents the

1. *Department of Mechanical Engineering, Sharif University of Technology, Tehran, Iran.*
*. *Corresponding author. E-mail: khayyat@mech.sharif.edu*

Received 3 April 2007; received in revised form 1 February 2008; accepted 26 February 2008

velocity prediction program and experimental results for the aerodynamic forces acting on the wing and the body of the land yacht. The VPP that is used in the present study is developed based on the static and dynamic characteristics of a land yacht [3,4]. It is the merit of a VPP application that it can provide not only global quantities like wing forces and moments but also detailed flow information useful for the design of a wing system. It is believed that VPP is a cost-effective tool for the performance prediction of a land yacht. Wind tunnel model tests are also carried out to measure the lift and drag of the wing system and the parasitic drag of the land yacht. Finally, VPP calculations are compared with experimental results to validate and explore the lift and drag changes due to various wing conditions. It should be noted that there are no similar studies for rigid wing or cloth sail land yachts.

MODEL SPECIFICATIONS

A radio controlled rigid wing land yacht model is used in the present study. This model is composed of two main sections: wing and body. The idea of a hard sail is a fairly new one and is still being refined. A NACA0012 airfoil is used for the hard sail. A balsa and basswood wing skeleton is used. The wooden skeleton is then covered with fiberglass.

The body has a conical form with the forward portion being like a half circle. A NACA0012 airfoil is also used for the rear axle of the land yacht. The angle of attack of the rear axle, with respect to true wind, is negative in order to produce a downward force, which increases the stability of the land yacht.

This land yacht is a radio controlled model that uses two electrical engines for the wing and the steering mechanism. These two electrical engines are controlled with a four channel radio controller. The servo motor of the wing is designed to help control the wing during wind shifts. Table 1 shows the technical specifications of the rigid wing land yacht model.

METHOD OF CALCULATION

The Velocity Prediction Program (VPP) has a two-part structure comprised of the land yacht model and the solution algorithm. The land yacht model is often thought of as a black box in which the land yacht speed is the input. The output is the difference between the aerodynamic drive force and the drag. It is then the job of the solution algorithm to find the drive force-drag equilibrium and to optimize the wing controls to produce the maximum speed at each true wind angle. There are two sets of parameters required to make a prediction: land yacht parameters and wing parameters. The aerodynamic simulation of the land

Table 1. Characteristics of the land yacht.

Land yacht weight	12.5 kg
Vertical wing span	1.2 m
Vertical wing chord line	0.5 m
Wing stall angle	12°
Front wheel diameter	0.1 m
Rear wheel diameter	0.2 m
Track	1.1 m
Wheel base	1.375 m
Rear axle wing chord line	0.1 m
Rear axle thickness	0.012 m
Vehicle fuselage drag coefficient	0.473
Coefficient of friction between wheels and road	0.75
Drag coefficient of rolling wheel, per wheel (B_W)	0.0136 kg/(rev/sec)

yacht is based on simple equations and experimental lift and drag coefficients. In the present study, we consider the motion of the land yacht, downwind and upwind, to keep the flow attached on the wing.

To understand how the VPP calculates aerodynamic forces and speed, one must understand what makes a land yacht go. The wind velocity triangle shown in Figure 1 consists of true wind (V_T) the wind caused by the land yacht speed (V_L) and the vector sum of the two or apparent wind (V_A). It is obvious that the wind velocity under which the wing operates is greater than the true wind speed.

The wing of the land yacht generates lift (F_L) and drag (F_D) from the apparent wind. The component of

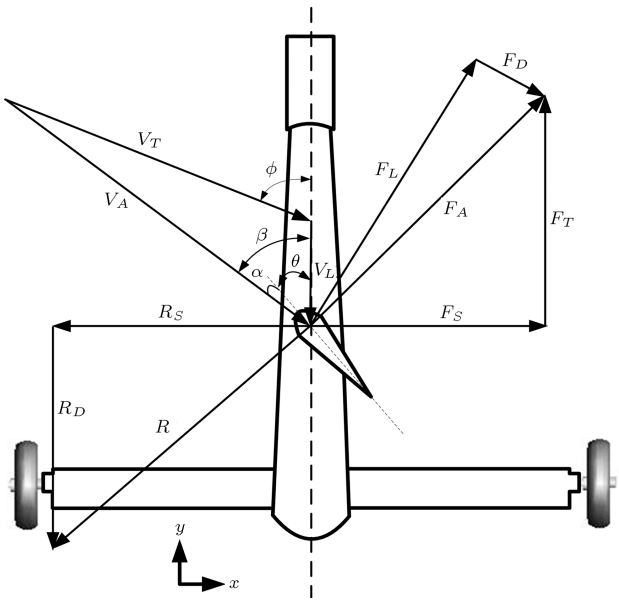

Figure 1. Aerodynamic force components.

the resulting aerodynamic force (F_A) in the direction of travel of the land yacht, is the drive force (F_T). This can be measured in the wind tunnel. The resultant aerodynamic force has a large component perpendicular to the direction of travel. This side force (F_S) must be resisted by the land yacht's wheel. When the wheels generate this equal and opposite side force (R_S) a drag force is also produced (R_D). When the thrust or drive force is equal to drag, the vehicle is in equilibrium and the maximum steady state speed has been reached. The equations of motion of the land yacht can be written as:

$$\begin{bmatrix}\cos(\theta+\alpha) & \sin(\theta+\alpha)\\ \sin(\theta+\alpha) & -\cos(\theta+\alpha)\end{bmatrix}\begin{pmatrix}F_L\\F_D\end{pmatrix}-\begin{pmatrix}R_S\\R_D\end{pmatrix}=\begin{pmatrix}m\ddot{x}\\m\ddot{y}\end{pmatrix}. \quad (1)$$

Here, $\ddot{x}$ and $\ddot{y}$ are the land yacht accelerations, respectively, in x and y directions, and R_D is the total drag force which is calculated by:

$$R_D = F_{DB} + F_{DA} + F_{DW}, \quad (2)$$

where:

F_{DB} = Drag force of body,
F_{DA} = Drag force of rear axle,
F_{DW} = Drag force of wheels.

The drag force of the body is calculated by:

$$F_{DB} = \frac{1}{2}\rho_{\text{air}} V_F^2 C_{DB} A_{PB}, \quad (3)$$

where A_{PB} is the total frontal fuselage projected area; C_{DB} is the vehicle fuselage drag coefficient and V_F is the apparent wind speed component in the travel direction of the land yacht that is calculated by:

$$V_F = V_A \times \cos\beta. \quad (4)$$

The drag force of the rear axle can be written as:

$$F_{DA} = \frac{1}{2}\rho_{\text{air}} V_F^2 C_{DA} A_{PA}, \quad (5)$$

where A_{PA} is the linear approximation to adjust the effective rear axle wing area based on angle of attack, and C_{DA} is the drag coefficient of rear axle wing. The drag force of the wheels can be expressed by:

$$F_{DW} = B_W(RPS_{FW} + 2RPS_{RW}), \quad (6)$$

where B_W is the drag coefficient of a rolling wheel and RPS_{FW} and RPS_{RW} are, respectively, calculated by:

$$RPS_{FW} = \frac{V_L}{\pi D_F}, \quad (7)$$

$$RPS_{RW} = \frac{V_L}{\pi D_R}, \quad (8)$$

where D_F is the front wheel diameter, and D_R is the rear wheel diameter.

The total available sideways friction force (R_S) is calculated by:

$$R_S = \mu \times F_{\text{Down}} = \mu \times (W + F_{LA}). \quad (9)$$

In Equation 9, μ is the coefficient of friction between the wheels and the road, W is the land yacht weight and F_{LA} is the lift force of the rear axle, which can be written as:

$$F_{LA} = \frac{1}{2}\rho_{\text{air}} V_F^2 C_{LA} A_{PA}, \quad (10)$$

where C_{LA} is the lift coefficient of rear axle wing.

The lift and drag forces, which are calculated by Equations 11 and 12, are functions of Reynolds number, wing angle of attack, camber and Mach number which are typically determined by the wind tunnel:

$$F_L = \frac{1}{2}\rho_{\text{air}} V_A^2 C_L A_W, \quad (11)$$

$$F_D = \frac{1}{2}\rho_{\text{air}} V_A^2 C_D A_W, \quad (12)$$

where A_W is the wing area.

When $\ddot{x} = 0$ and $\ddot{y} = 0$, the land yacht is in equilibrium and its maximum steady state speed has been reached. From the VPP [4], the forces and velocity can be solved for simultaneous equations or an iterative process involving guessing the land yacht speed until $\ddot{x}$ and $\ddot{y}$ are equal to zero.

EXPERIMENTAL METHOD

The experiments are carried out in the national open jet wind tunnel of Malek Ashtar University of Technology in Iran. This wind tunnel is a low speed tunnel which operates in a Sub-Sonic regime. The air stream in the open test section is free to expand, therefore, the wake and solid-blockage effect are very small [5]. The dimensions of the test section are 2.2 m high and 2.8 m wide and the wind tunnel speed is 100 m/s at a maximum condition. A three-component force balance is located under the wind tunnel stand, the dimensions of which are 2 m ×3 m, which is used to simulate the ground effects. The test specimen is attached to a rigid rod and the rod is fastened into the load cells, which can be turned to change the apparent wind angle so that the forces are measured in a coordinate system aligned with the centerline of the model and the horizontal plane. A potentiometer in the load cell is used to measure the angle of attack. Special software is used to translate the voltage measurements made by the load

cells into force units of kilograms. The calibration rod and weight are used to determine the voltage associated with a given force [6] and the calibration results are shown in Table 2. Measurement of lift and drag is carried out for wind speed 9 $\frac{\text{m}}{\text{s}}$ at various apparent wind angles. The wind tunnel is also equipped with a Pitot tube, which allows the downstream velocity to be measured. The Pitot tube measures the pressure in units of height of oil. The velocity is then measured graphically [7].

The full size of a radio controlled rigid wing land yacht, comprised of wing, body frame, rear axle and wheels, is selected for the wind tunnel testing. The model can be rotated about a fixed axis at its centerline. Wind tunnel tests are conducted in three stages: body testing without the wing and wing testing with the body and without the body at various apparent wind angles between ($0^\circ - 150^\circ$). At each of the apparent wind angles, the wing doing an α (wing angle of attack) will sweep from 0° to 90° in increments of 3°. An approximate logarithmic vertical velocity profile in the onset flow is achieved by placing a trip board in the wind tunnel upstream of the test section. The velocity change over the span of the sails is about 5%. This profile is used for all tests. The reference flow velocity is about 9 m/s. The reference height for defining the apparent wind angle and velocity is taken as the geometric centre of the wing area height.

LIFT AND DRAG COEFFICIENTS

In the wind tunnel, the thrust force (F_T) and side force (F_S) created by the wing are measured in a horizontal plane, where the thrust force is parallel to the centerline of the land yacht and the side force perpendicular to it. The vertical force (F_Z) is positive upwards. F_Z in body fixed coordinates is here referred to as the force acting upon the wing. In this description, the wing bend and deflection are ignored and the wing is assumed to be aligned with the z-axis. The drag force (F_D) is defined as the force in line with the onset flow, and lift force (F_L) as being perpendicular to it. As shown in Figure 1, the lift and drag can be obtained from F_T and F_S by rotating the coordinate system through the apparent wind angle with:

$$\begin{pmatrix} F_L \\ F_D \end{pmatrix} = \begin{bmatrix} \sin(\beta) & \cos(\beta) \\ -\cos(\beta) & \sin(\beta) \end{bmatrix} \begin{pmatrix} F_T \\ F_S \end{pmatrix}. \tag{13}$$

It is convenient to write forces in a non-dimensional coefficient form.

The total drag is the sum of the induced drag and the viscous drag [8]. In a coefficient form, it can be written as:

$$C_D = C_{Dvis} + C_{Di} = C_{Dvis} + \frac{C_L^2}{\pi\ e\ AR}. \tag{14}$$

The induced drag, C_{Di}, is ideally a function of the lift coefficient squared and depends on the aspect ratio (AR) and e is Oswald's efficiency factor. The viscous drag coefficient, C_{Dvis}, consists of the skin friction and separation drag, which cannot easily be separated [8]. As mentioned before, a NACA0012 airfoil that is used for the hard sail of a land yacht is our test specimen. Figure 2 shows the characteristics of the wing that are obtained from the wind tunnel (Configuration 0) in comparison with published values until the stall point (Configuration 1) [9].

Conventionally, experimental results are determined under discrete conditions, whilst the VPP requires a continuous definition of behavior [10]. To take this step, some form of regression analysis must be performed to derive the coefficients in an equation that describes land yacht behavior. This is done by curve fitting the wind tunnel drag versus lift data with the parabolic drag equation:

Table 2. Wind tunnel load cell calibration results.

Test No.	Real Weight (gr)	Measured Weight by Load Cell (kg)	Error
1	98	0.1	2%
2	496	0.49	1.2%
3	987	0.99	0.3%
4	1984	1.99	0.3%
5	4984	5	0.3%

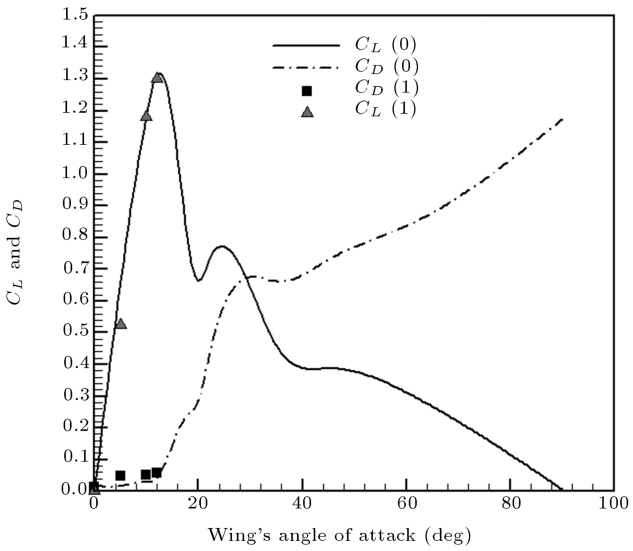

Figure 2. C_L and C_D versus wing angle of attack for a NACA 0012 wing at Re $= 3 \times 10^5$.

$$C_D = C_{D0} + K_i C_L^2. \tag{15}$$

From the curve fitting shown in Figure 3, C_{D0} and K_i are 0.014 and 0.139, respectively. The Oswald factor, calculated by Equation 16, is 0.954.

$$e = \frac{1}{K_i\ \pi\ AR}. \tag{16}$$

With this accomplished, the VPP outputs the velocity curves, representing the land yacht velocity and course, relative to the true wind direction, respectively.

PARASITIC DRAG OF THE MODEL

The parasitic drag of the model is determined by measuring the forces acting on the land yacht without the wing. Measurements are conducted for the upwind and downwind test configuration to ensure that the effect of twist profiles is correctly accounted for. Six different sets of tests are done. These tests consist of changing the body angle, with respect to air flow, in a horizontal plane. These angles are 0°, 30°, 45°, 90°, 135°and 150°. All of the tests are done at a tunnel speed of 9 m/s. The total horizontal parasitic drag (R_D) measured in the wind tunnel is approximately similar to that predicted by the VPP. This comparison is shown in Figure 4. In order to calculate the total frontal fuselage projected area of the body (A_{PB}) and the effective rear axle wing area (A_{PA}), which are used in the VPP code, the body and the rear axle of the land yacht are exactly modeled by Mechanical Desktop software (MDT). This software calculates the effective area of the body and the rear axle at any apparent wind angle.

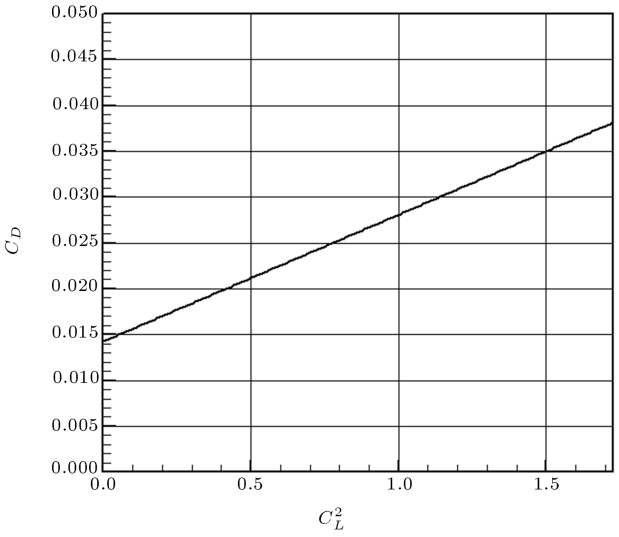

Figure 3. C_D versus C_L^2 for a NACA 0012 wing.

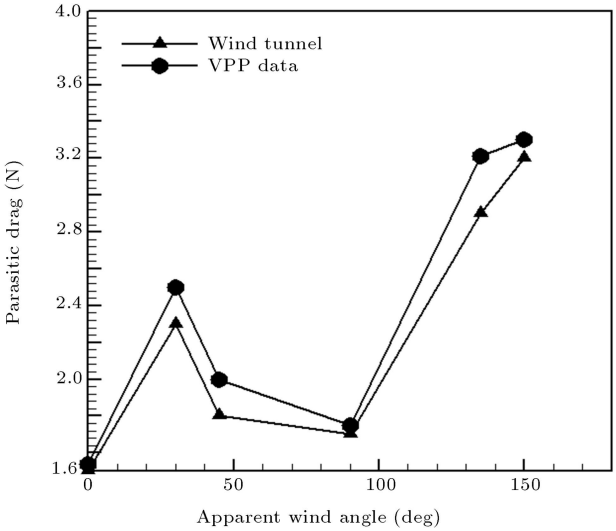

Figure 4. Parasitic drag of model in horizontal plane and predicted by the VPP at tunnel speed of 9 m/s.

ERROR ANALYSIS

The accuracy of the pressure transducer used introduces an error in the measurements. This accuracy, as reported by the manufacturer, is 0.25% FS (0.0005 in of water). The error calculation in the pressure coefficients is based on RSS (Root Sum of Squares) type uncertainty [11].

A sample calculation and a sample table for errors in the pressure coefficient for Re = 30218, where dynamic pressure (q) values were lowest and $\alpha = 15°$, are shown here.

For specific pressure coefficient, C_p, and dynamic pressure q, we have:

$$C_p = \frac{\Delta P}{q} = \frac{P - P_S}{q}, \tag{17}$$

where:

P = Pressure being measured (upper or lower surface pressure),
P_S = Static pressure,
q = Dynamic pressure,

$$\delta C_P = \sqrt{\left[\frac{\partial C_P}{\partial(\Delta P)} \times \delta(\Delta P)\right]^2 + \left[\frac{\partial C_P}{\partial q} \times \delta(q)\right]^2}. \tag{18}$$

Here, $\delta(\Delta P) = \delta(q) = 0.0005$, which is the accuracy of the pressure transducer. Table 3 shows a sample set of errors calculated in the pressure coefficients. So, for a particular pressure measurement, we can obtain the error in the pressure coefficient. The error in the pressure coefficient calculation introduces error in the local lift coefficient calculation. This was also based on

Table 3. Error in pressure coefficients for Re = 30218 and $\alpha = 15°$.

Error Calculation in Pressure Coefficients.					
Upper Surface			Lower Surface		
Port No.	$C_{P.U}$	Error in $C_{P.U}$	Port No.	$C_{P.L}$	Error in $C_{P.L}$
1	-0.08	0.042	1	-0.08	0.042
2	-0.75	0.052	13	0.58	0.048
3	-0.75	0.052	14	0.25	0.043
4	-0.75	0.052	15	0.17	0.042
5	-0.75	0.052	16	0.08	0.042
6	-0.75	0.052	17	0.08	0.042
7	-0.50	0.047	18	0.08	0.042
8	-0.17	0.042	19	0.08	0.042
9	-0.17	0.042	20	0.08	0.042
10	-0.08	0.042	21	0.08	0.042
11	-0.08	0.042	22	0.08	0.042
12	0.00	0.042	23	0.00	0.042

RSS type uncertainty. The error in C_L is then given as:

$$\delta C_L = \sum (\delta C_{P.U} - \delta C_{P.L}). \tag{19}$$

The maximum error was found for the data at Re = 30218, where dynamic pressure (q) values were lowest, resulting in a higher error in the pressures measured. This maximum error in the pressure coefficients was found to be of the order of ± 3.5%. Error in the total lift coefficient obtained from the pressure measurements was about ± 1.2%. Errors in other readings were found to be lower than these. The error in the angle of attack measurement for the pressure measurement setup is ± 0.05°. The error in the angle of attack measurements for lift measurements using a force balance is ± 0.01°.

COMPARISON OF AERODYNAMIC FORCES

In the wind tunnel, it is possible to try a number of different land yacht situations with respect to air flow to find the 'optimal' setting for each sailing condition. The wing is adjusted in the wind tunnel to maximize the drive force coefficient (C_{Thrust}) in order to approximate the optimal lift and drag coefficients for each test condition. The drive force and sideways force coefficients for the land yacht are measured for five different cases. In each of these cases, the angle of the body, with respect to the oncoming wind, and the wing angle of attack are varied independently from each other and the lift and drag forces of the wing are measured. In fact, drive force coefficient (C_{Thrust}) and sideways force coefficient (C_{Sideways}) are calculated from the lift and drag coefficients of the wing by:

$$\begin{cases} C_{\text{Sideways}} = C_L \cos(\beta) + C_D \sin(\beta) \\ C_{\text{Thrust}} = C_L \sin(\beta) - C_D \cos(\beta) \end{cases} \tag{20}$$

The angles of the body, with respect to the wind, are: 30°, 45°, 90°, 135° and 150°. At each of these angles, the wing angle of attack changes from 0° to 90°. The wing forces that are measured include the interaction effect between the body and the wing.

As shown in Figure 5, land yachts can sail on different courses. In a closed hauled course, the land yacht goes windward under an angle [12]. Therefore, this course occurs when the angle of the body, with respect to the wind, is smaller than 90°. The drive and sideways force coefficients versus the wing angle of attack, for body angles of 30° and 45°, are depicted in Figures 6 and 7, respectively. It will be evident from these figures that on this particular course, a land yacht produces only a little drive force when compared to the total sideways pointed force. When the drag vector thrust component cancels out the thrust component of the lift vector, the land yacht is experiencing zero thrust. The wing of the land yacht also experiences something else; it experiences a decrease in magnitude of the lift vector, even all the way up to 0, when the angle of attack of the airflow is decreasing into smaller and smaller angles or even zero. The drag vector often levels off at some magnitude. This phenomenon could limit the top speed of a land yacht.

When the angle of the body with respect to wind is 90° the land yacht is sailing on a beam reach course [12]. In this course, when the land yacht begins

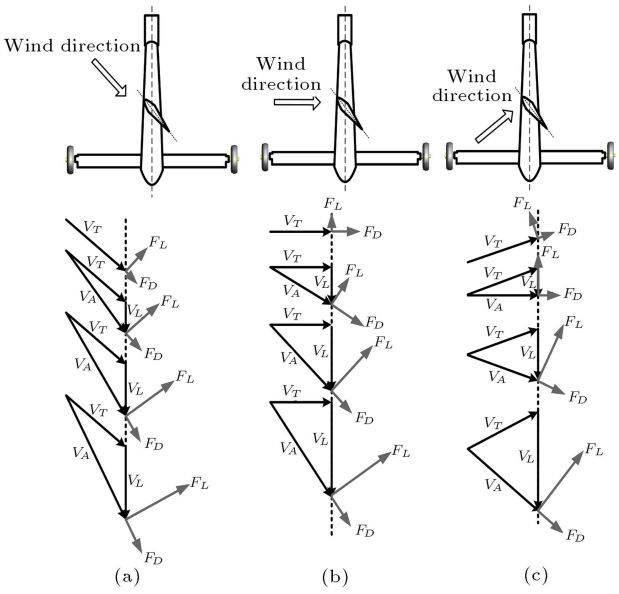

Figure 5. Lift and drag diagram of the vertical wing at various true wind angles.

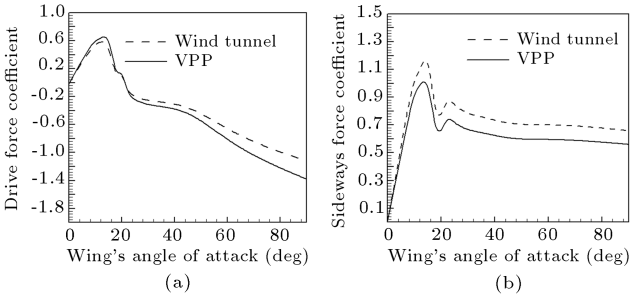

Figure 6. Aerodynamic coefficients obtained by testing the land yacht model in the wind tunnel and the VPP code at the body angle of 30° with respect to the wind: (a) Drive force coefficient; (b) Sideways force coefficient.

to move, the drive force will be equal to the lift force of the wing. Figure 8 shows the drive and sideways force coefficients versus wing angle of attack for this particular course. In a small wing angle of attack, the drive force is greater than the total sideways force. This is converse when the angle of attack increases. In a beam reach course, the wing will behave very much as it would on a closed hauled course. With the absence of the drop off of thrust, which is encountered on a close hauled course, the drop off still occurs, but only at very high wing angles of attack. This course is known for its higher thrust vector magnitudes at given speeds. The beam reach is just a course which strikes an optimum between several positive and negative effects competing with each other.

Finally, when the angle of the body, with respect to wind, is greater than 90°, the land yacht goes downwind [12]. This is known as a broad reach course. Figures 9 and 10 show the drive and sideways force

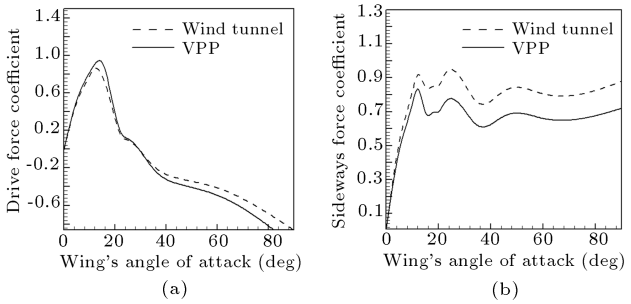

Figure 7. Aerodynamic coefficients obtained by testing the land yacht model in the wind tunnel and the VPP code at the body angle of 45° with respect to the wind: (a) Drive force coefficient; (b) Sideways force coefficient.

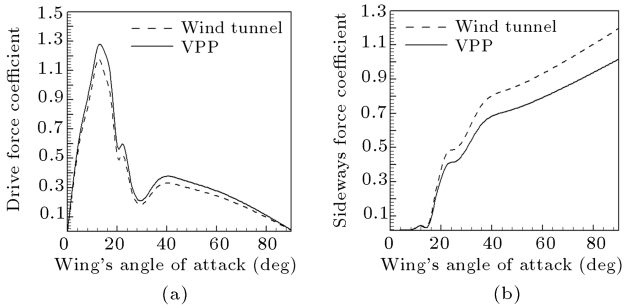

Figure 8. Aerodynamic coefficients obtained by testing the land yacht model in the wind tunnel and the VPP code at the body angle of 90° with respect to the wind: (a) Drive force coefficient; (b) Sideways force coefficient.

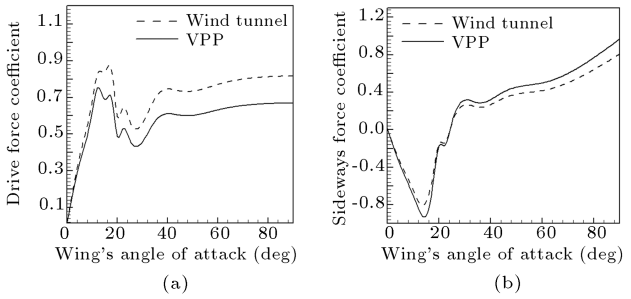

Figure 9. Aerodynamic coefficients obtained by testing the land yacht model in the wind tunnel and the VPP code at the body angle of 135° with respect to the wind: (a) Drive force coefficient; (b) Sideways force coefficient.

coefficient versus wing angle of attack for the body angles of 135° and 150°, respectively. It is evident from these figures that on this particular course, a land yacht produces only a little sideways force when compared to the drive force. All courses that have a greater angle than 90° with respect to wind, have a thrust dip. A thrust dip is the name for the phenomenon wherein from zero speed, the thrust decreases until a certain land yacht velocity and only then starts to rise.

In our study, the tests are carried out at a tunnel speed of 9 m/s. This speed is greater than the speed

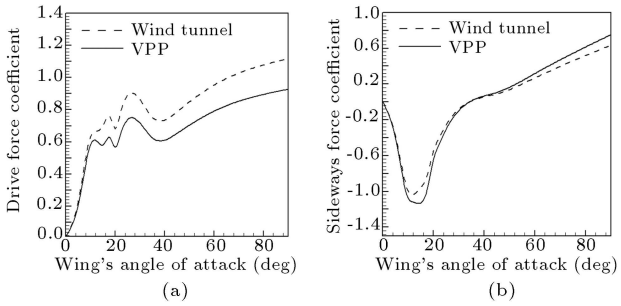

Figure 10. Aerodynamic coefficients obtained by testing the land yacht model in the wind tunnel and theVPP code at the body angle of 150° with respect to the wind: (a) Drive force coefficient; (b) Sideways force coefficient

at which the thrust dip happens. Therefore, the thrust dip cannot be seen in Figures 9 and 10. It should be noted that at this particular course, the drag vector, as the lift vector, is producing a drive force. Therefore, when the wing angle of attack increases, the drive force increases too. It is possible to reach high speeds on broad reaches, but this all comes down to how capable you and your land yacht are in overcoming the thrust dip and maintaining the acquired speed (thus preventing falling back into the dip).

Now, the discrepancy in aerodynamic force between the VPP data set and the wind tunnel measurements can be explained as follows: (a) In the experiments, some equipment such as shrouds to support the wing are used, but they are not found in the present VPP calculation. It could provide an additional drag in experiments. We know that in a closed hauled and beam reach course, the drag vector thrust component cancels out the thrust, and the drag vector sideways component produces the sideways force. Therefore, in these courses, the drive force coefficient obtained by the wind tunnel is smaller than either in the VPP, until the thrust force becomes equal to zero; this subsequently reverses. Also, the sideways force coefficient obtained by the wind tunnel is greater than either in the VPP. In a broad reach course or in downwind sailing, the drag vector sideways component cancels out the sideways force and the drag vector thrust component produces the drive force. Therefore, in these courses, the drive force coefficient obtained by the wind tunnel is greater than either in the VPP. Also, the sideways force coefficient obtained by the wind tunnel is greater than either in the VPP, until the sideways force becomes equal to zero; this subsequently reverses; (b) After the stall point, the VPP calculates the lift coefficient by:

$$C_L = (3.08 \times 10^{-7})\alpha^4 - (6.92 \times 10^{-5})\alpha^3 + (5.49 \times 10^{-3})\alpha^2 - 0.19\alpha + 2.9, \quad (21)$$

where α is the wing angle of attack (deg).

Equation 21 is derived by curve fitting the wind tunnel lift data versus the wing angle of attack after the stall point (12°) and approximately estimates the lift coefficient behavior after this point. But, this estimation is not very exact. Therefore, after the stalling point, the discrepancy between the VPP data set and the wind tunnel measurements is greater than either before the stalling point.

OPTIMAL POINT FOR THE BEGINNING OF THE MOVEMENT

In general, a land yacht tends to move in the resultant aerodynamic force (F_A) direction, but the friction force of the wheels causes resistance and tends to move the land yacht in a travel direction. Thus, it is better that the angle between F_A and V_L be small because the aerodynamic force will be more aligned with the travel direction. Now, when the angle between F_A and V_L is tending to zero, it means $\varepsilon = 0$ (F_A is equal to thrust). Figure 11 shows the different cases for the beginning of the movement.

From Figure 11b, the thrust force can be written as:

$$F_T = F_L \cos\lambda + F_D \sin\lambda = F_A \cos\varepsilon. \quad (22)$$

When $\lambda = 0$, as shown in Figure 11a, the thrust force will be equal to the lift force of the wing. In order to find the maximum value of the thrust force, the derivative of F_T with respect to λ must be calculated. If $\frac{\partial F_T}{\partial \lambda} = 0$, it will be shown that:

$$\lambda = \arctan\left(\frac{F_D}{F_L}\right). \quad (23)$$

For this value of λ, the thrust force will be maximized. Figure 12 shows the schematic variation of F_T, with respect to $\cos\lambda$. From this figure, it is evident that when $\frac{F_L^2 - F_D^2}{F_L^2 + F_D^2} < \cos\lambda < 1$, then the thrust force that is shown in Figure 11a, will be smaller than either in Figure 11b.

In our studies, the wind tunnel data set can help to find the optimal angle of the body, with respect to

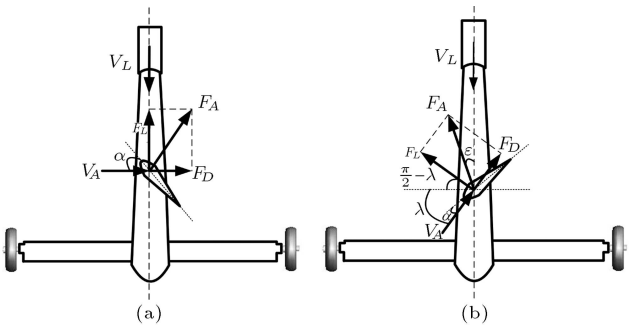

Figure 11. Various starting points of the land yacht movement: (a) Apparent wind angle = 90; (b) Apparent wind angle > 90.

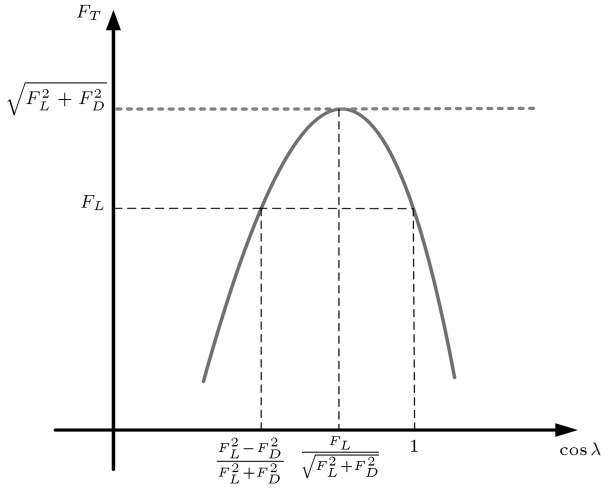

Figure 12. Schematic variation of drive force with respect to $\cos\lambda$.

wind, at the beginning of the movement. Figure 13 shows the drive force coefficients obtained by the wind tunnel at different angles of the body, with respect to wind. From this figure, it is evident that the maximum drive force occurs when the angle of the body, with respect to wind, is equal to 90° and the wing angle of attack is about 12°. This result also can be obtained from the VPP.

LAND YACHT ROAD TEST

To examine the accuracy of the VPP [13], the real speed of the land yacht is measured by using a cycle computer and is compared with the VPP data. This device measures the model speed accurately. This speedometer has a sensor and a magnet. The magnet is mounted on the rear wheel and the sensor is mounted on the rear axle at a certain distance from the magnet. The center of the magnet must be aligned to either of the sensor's marking lines. When the land yacht moves, the magnet observes the sensor and each time sends an electrical pulse to the small board that exists in the cycle computer; this board determines the rotational speed of the wheel. By multiplying this speed to the radius upon which that magnet is mounted, the linear speed of that point and finally the speed of the land yacht are achieved. This cycle computer shows the current speed, trip distance, maximum speed, average speed and elapsed time. Figure 14 shows the maximum speed of the land yacht at different true wind speeds for both real and VPP data. The computed results show reasonably good agreement in comparison with the real speed obtained from the land yacht road test.

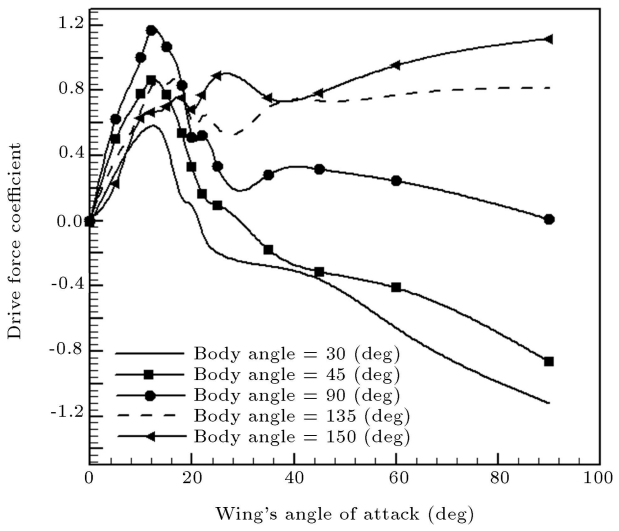

Figure 13. Drive force coefficient versus wing angle of attack at different body angles.

CONCLUSION

The wind tunnel is a helpful tool for determining a land yacht's expected performance. Towards the ultimate goal, which is to make land yachts faster, wind tunnel results (in combination with analytical tools, such as a VPP) can be utilized to achieve results faster and more safely than the trial and error methods used today. The computed results show reasonably good agreement in comparison with the experimental data obtained from the wind tunnel test. It is quite certain that VPP can be a very powerful and useful tool for the aerodynamic performance prediction of land yachts at the basic design stage if the wing lift and drag coefficients are determined accurately.

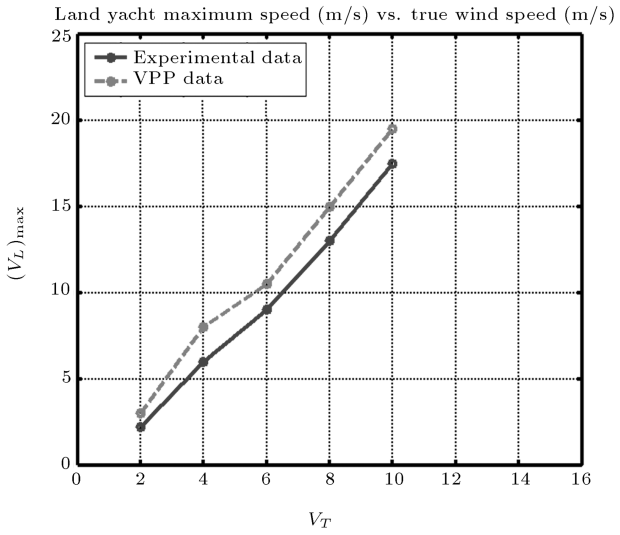

Figure 14. Maximum speed of the land yacht at various true wind speeds obtained by testing the land yacht model and the VPP.

ACKNOWLEDGMENTS

This research has benefitted from the support of the Malek Ashtar University of Technology. The authors would like to acknowledge the contributions of Adel Abedian, Jafar Gol Mohammadi and Abbas Ashrafi to this work.

REFERENCES

1. Kerwin, J.E. and Newman, J.N. "A summary of the H. Irving Pratt ocean race handicapping project", *Proceedings of the 4th CSYS*, Annapolis, MD, USA (1979).
2. Hazen, G.S. "A model of sail aerodynamics for diverse rig types", *Proceedings of New England Sailing Yacht Symposium* (1980).
3. Parr, A., *Sand Yachting*, 3rd Ed., Gomer Press (2001).
4. Khayyat, M. and Rad, M. "Land yacht aerodynamic performance", *Proceedings of the 13th Annual International Conference on Mechanical Engineering, ISME*, Isfahan, Iran (17-19 May 2005).
5. Mueller, T.J. and Jansen, B.S., Jr. "Aerodynamic measurements at low Reynolds number", *AIAA Paper 82-0598, Presented at the Twelfth Aerodynamic Testing Conference*, Williamsburg, VA (1982).
6. Barlow, J.B. et al., *Low-Speed Wind Tunnel Testing*, 3rd Ed., John Wiley & Sons, Inc. (1999).
7. Spaulding, E.R. and Merriam, K.G. "Comparative tests of pitot-static tubes", *NACA TN 546*, pp. 1-5 and 32 (Nov. 1935).
8. Ockendon, H. and Ockendon, J.R., *Viscous Flow*, Cambridge University Press, Cambridge (1995).
9. Smith, M.J. et al. "Performance analysis of a wing with multiple winglets", *AIAA-2001-2407 Applied Aerodynamics Conference*, 19th, Anaheim, CA (11-14 June 2001).
10. Van Oossanen, P. "Predicting the speed of sailing yachts", *Transactions of the Society of Naval Architects and Marine Engineers*, **101**, pp. 337-397 (1993).
11. AIAA Standard "Assessment of wind tunnel data uncertainty", AIAA S-071-1995, Washington D.C. (1995).
12. Marchaj, C.A., *Sailing Theory and Practice*, Adlard Coles Limited, London (1907).
13. Davidson, K.S.M. "Some experimental studies of the sailing yacht", *Transactions of the Society of Naval Architects and Marine Engineers*, **44**, pp. 441-453 (1936).